Carbon isotope stratigraphy across the Permian/Triassic boundary at Jolfa (NW-Iran), Peitlerkofel (Sas de Pütia, Sass de Putia), Pufels (Bula, Bulla), Tesero (all three Southern Alps, Italy) and Gerennavár (Bükk Mts., Hungary)

By

CHRISTOPH KORTE & HEINZ W. KOZUR

with 7 figures and 1 table

Key words:
Carbon isotope stratigraphy
Permian/Triassic boundary
Jolfa (Iran)
Southern Alps (Italy)
Gerennavár (Bükk Mts., Hungary)

Addresses of the authors:
CHRISTOPH KORTE
Institut für Geologie und Paläontologie
Universität Innsbruck
Innrain 52
A-6020 Innsbruck
Austria
present email: christoph.korte@earth.ox.ac.uk

HEINZ W. KOZUR
Rézsü u. 83
H-1029 Budapest
Hungary
kozurh@helka.iif.hu

Journal of Alpine Geology **Mitt. Ges. Geol. Bergbaustud. Österr.**	**47**	**S. 119-135**	**Wien 2005**

Contents

Abstract

High resolution carbon isotope curves are documented for five Permian/Triassic boundary sections: Kuh-e-Ali Bashi near Jolfa (NW-Iran), Peitlerkofel (Sas de Pütia, Sass de Putia), Pufels (Bula, Bulla), Tesero (all three Southern Alps, Italy) and Gerennavár (Bükk Mts., Hungary).

The Dorashamian sediments of the Jolfa section were deposited in an open marine environment with water depths in excess of 60 meters. All conodont zones are present, and the section marks therefore a complete biostratigraphic Permian/Triassic transition. The decline of the $\delta^{13}C$ values starts at ~ 3 ‰ in the *C. nodosa* Zone, reaching ~ 0.3 ‰ at the top of the *C. hauschkei* Zone and ~ -1.6 ‰ in the lower *H. parvus* Zone, followed by an increase in the upper *H. parvus* and lower *I. isarcica* Zones to -0.5 ‰.

The Permian/Triassic boundary sections of the Southern Alps and the Gerennavár (Bükk Mts., Hungary) were compared with each other and with the previously published Seis (Siusi) and San Antonio sections, using the 2 and 0 ‰ chemostratigraphic levels. At Pufels and Tesero the 2 ‰ level is crossed at the top of the Bellerophon Limestone, but at Peitlerkofel this chemostratigraphic level is 40 cm below the top of the Bellerophon Limestone and thus lithostratigraphically lower. In each section the $\delta^{13}C$ decline continues and 0 ‰ is reached at the top of the Oolite Horizon at Tesero, but at Pufels and Peitlerkofel lithostratigraphical higher within the lower Mazzin Member. At the more marginal Seis section both, the 2 and the 0 ‰ chemostratigraphic levels lie within the Tesero Oolite facies, hence this facies begins earlier and ranges higher up than in the more basinal sections in the E-NE. At the more basinal sections San Antonio and Gerennavár the 2 ‰ chemostratigraphic level lies within the upper Bellerophon Limestone and within the upper Nagyvisnyó Formation, respectively. In both sections the equivalent of the lower Tesero Oolite Horizon of the Western Dolomites is replaced by the fossil-rich dark bioclastic limestones of the Badiota facies of the Bellerophon Limestone Formation (=Nagyvisnyó Formation at Gerennavár). The equivalent of the middle and upper Tesero Oolite Horizon of western Dolomites is replaced by the basinal facies of the Mazzin Member (=Gerennavár Limestone Formation at Gerennavár). At Gerennavár a distinct Boundary Clay is intercalated between the Nagyvisnyó Formation and the Gerennavár Limestone Formation. The mass extinction at the base of this Boundary Clay can be correlated with the event boundary of the pelagic PTB sections in Iran and China.

The carbon isotope curves of the Southern Alps suggest that the lithologic changes from the Tesero oolite to the Mazzin Member from the Bellerophon Limestone to the Tesero oolite and are diachronous. Previously, the last facies transition was regarded to be synchronous with the Permian/Triassic boundary.

1. Introduction

The Permian/Triassic boundary (PTB) was marked by the largest mass extinction of the entire Phanerozoic history that affected marine and continental biota (e.g. SCHINDEWOLF 1953, SEPKOSKI 1989, RAUP 1991, ERWIN 1993, KOZUR 1998a, 1998b). This severe event was accompanied by distinct changes in isotope records. The seawater $^{87}Sr/^{86}Sr$ and $\delta^{34}S$ rose rapidly (HOLSER & KAPLAN 1966, VEIZER & COMPSTON 1974, CLAYPOOL et al. 1980, BURKE et al. 1982, KOEPNICK et al. 1990, MARTIN & MACDOUGALL 1995, VEIZER et al. 1999, KORTE et al. 2003, 2004a, NEWTON et al. 2004). A negative carbon isotope excursion was documented for marine carbonates (MAGARITZ et al. 1988, HOLSER et al. 1989, OBERHÄNSLI et al. 1989, CHEN et al. 1991, JIN et al. 2000, DOLENEC et al. 2001, KORTE et al. 2004a) as well as for marine and terrestrial organic material (WANG et al. 1994, WIGNALL et al. 1998, HANSEN et al. 2000, MUSASHI et al. 2001, DE WIT et al. 2002). Due to its wide regional expression the excursion can be regarded as a global secular trend (BAUD et al. 1989) that was attributed to a variety of causes. For example, a massive re-oxidation of previously stored ^{12}C-enriched organic material, due to eustatic regression (BAUD et al. 1989, HOLSER & MAGARITZ 1992), or a release of isotopic light oceanic methane hydrates (ERWIN 1993, MORANTE 1996, KRULL et al. 2000, DE WIT et al. 2002) could be the cause, but the decline in $\delta^{13}C$ is gradual, covering a protracted time interval (MAGARITZ et al. 1988, HOLSER et al. 1989, KORTE et al. 2004a, 2004b, 2004c), making these short-term events

improbable explanations. Other scenarios argue for a breakdown in oceanic primary productivity (VISSCHER et al. 1996) that disturbed the biological pump (HOLSER 1997). Siberian Trap volcanism (RENNE et al. 1995, BERNER 2002), or oceanic overturn that resulted upwelling of (anoxic) bottom waters (KNOLL et al. 1996, KORTE et al. 2004a) may also contribute to the negative carbon isotope excursion (see ERWIN et al. 2002, KUMP 2003 for further information).

Based on carbon isotope records for the Iranian PTB sections at Abadeh and Shahreza HEYDARI et al. (2001) postulated that the negative $\delta^{13}C$ excursion, and the covariance of the carbon and oxygen isotope values, were generated, at least in part, by meteoric diagenesis during subaerial exposure of sediments. However, KORTE et al. (2004a) pointed out that the Dorashamian and the lowermost Triassic sediments at Abadeh represent a complete biostratigraphical succession, the $\delta^{13}C$ decrease in the upper Dorashamian rocks is gradual, and the coeval water depth was in excess of 60 m. Moreover, for the time interval that contains the negative carbon isotope shift no correlation exists between $\delta^{13}C$ and $\delta^{18}O$. The negative carbon isotope excursions in continuous marine sections can therefore be regarded as a primary secular signal.

In this study we present whole rock carbonate $\delta^{13}C$ values for five Permian/Triassic boundary successions, Kuh-e-Ali Bashi near Jolfa (NW-Iran), Peitlerkofel (Sas de Pütia, Sass de Putia), Pufels (Bula, Bulla), Tesero (all three Southern Alps), and Gerennavár (Bükk Mts., Hungary), and utilise their isotope curves as a stratigraphic tool.

2. Geological settings

2.1. Jolfa (NW-Iran)

The Late Permian and Early Triassic Kuh-e-Ali Bashi succession at Jolfa (NW-Iran) (Figs. 1 and 2) was deposited on the shelf of the Sanandaj-Sirjan block, a part of the Cimmerian microcontinent, under open marine tropical conditions about 1000 km north of the tropic of Capricorn (STAMPFLI & BOREL 2002). Its biostratigraphic constraints were discussed by several authors (e.g. STEPANOV et al. 1969, TEICHERT et al. 1973, KOZUR et al. 1975, 1978, SWEET & MEI 1999a, 1999b, KOZUR 2004, and in press). In the Jolfa sections, on the slope of the main valley at Kuh-e-Ali Bashi (Fig. 1), a continuous sequence from the upper Khachik Formation (late Capitanian) to the Early Triassic *I. isarcica* Zone of the Elikah Formation, are exposed. The rock material was sampled by H.W.K. in 1998 from gullies on the slope of this valley. These localities are different from those of TEICHERT et al. (1973), which were also re-sampled by H.W.K. in 2002. The Dorashamian Alibashi Formation (sensu TEICHERT et al. 1973) comprises reddish pelagic limestones, marls and shales. It is underlain by reddish limestones of the upper Jolfa Formation (upper Dzhulfian) and overlain by the Elikah Formation which starts with the Boundary Clay of the uppermost Dorashamian (*C. meishanensis-H. praeparvus* Zone) and continues into the Triassic (*H. parvus* and *I. isarcica* Zones and younger Early Triassic). The Alibashi Formation begins with reddish shales, marls and limestones of the *Phisonites* beds and ends either with the *Paratirolites* Limestone (section 4 sensu TEICHERT et al. 1973) or encompasses also the Boundary Clay composed of shales, marls, and overlying thin marly limestones (section 1 sensu TEICHERT et al., 1973). TEICHERT et al. (1973) reported for their locality 4 pale red, greyish red, red, and reddish colours as typical for the pelagic limestones and shales of the Dorashamian Alibashi Formation. The upper 12 m of the 16.5 m of this section contain *Paratirolites*, a guideform for the upper Dorashamian. Other Dorashamian fossils, like the brachiopod *Araxathyris araxensis minor* and deep-water rugose corals and nautiloids are present.

SWEET (in TEICHERT et al. 1973) correctly determined the conodonts of their section 4 (their samples Sc 1, 2, 5, 6, 7L, 7M and 7U) as Dorashamian = Changxingian (mentioning both names) and established the Dorashamian guideform *Clarkina subcarinata* s.l. At that time, other Dorashamian gondolellid species, such as *C. changxingensis* (WANG & WANG) and *C. deflecta* (WANG & WANG), were still regarded as *C. subcarinata* and only several years later separated into independent taxa. Re-examination (H.W.K.) of the Iranian conodont collections of Sweet (from TEICHERT et al. 1973) revealed that the Jolfa samples Sc 1, Sc 2, Sc 5 from locality 4 of TEICHERT et al. (1973) contain the lower to middle Dorashamian guideform *C. subcarinata*, samples Sc 5, Sc 6 and Sc 7L the middle to upper Dorashamian guideforms *C. changxingensis* and partly also *C. deflecta*, and in the youngest sample Sc 7U (10 cm below the top of the *Paratirolites* Limestone) *C. iranica* (KOZUR 2004) and *C. sosioensis* are present. Thus, the Dorashamian, from the *C. subcarinata* Zone up to the *C. iranica* Zone, is represented within Sweet's conodonts of locality 4 of the Alibashi Formation. At locality 1 (sensu TEICHERT et al. 1973) the entire Dorashamian, from its base up to 1.1 m above the *Paratirolites* Limestone (including the Boundary Clay with the *C. meishanensis-H. praeparvus* Zone), was assigned to the Alibashi Formation. In this section, there is an overlap between the Alibashi Formation and the basal part of the Elikah Formation (the latter generally starts with the Boundary Clay). The sharp lithologic boundary at the base of the Boundary Clay is the natural base of the Elikah Formation.

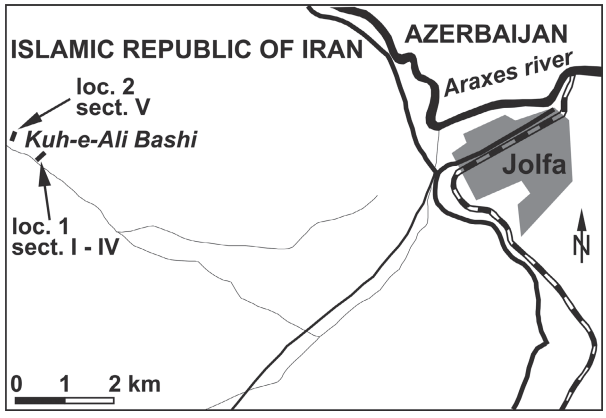

Fig. 1: Locations of the investigated sections of the Permian/Triassic boundary successions at Jolfa, NW-Iran.

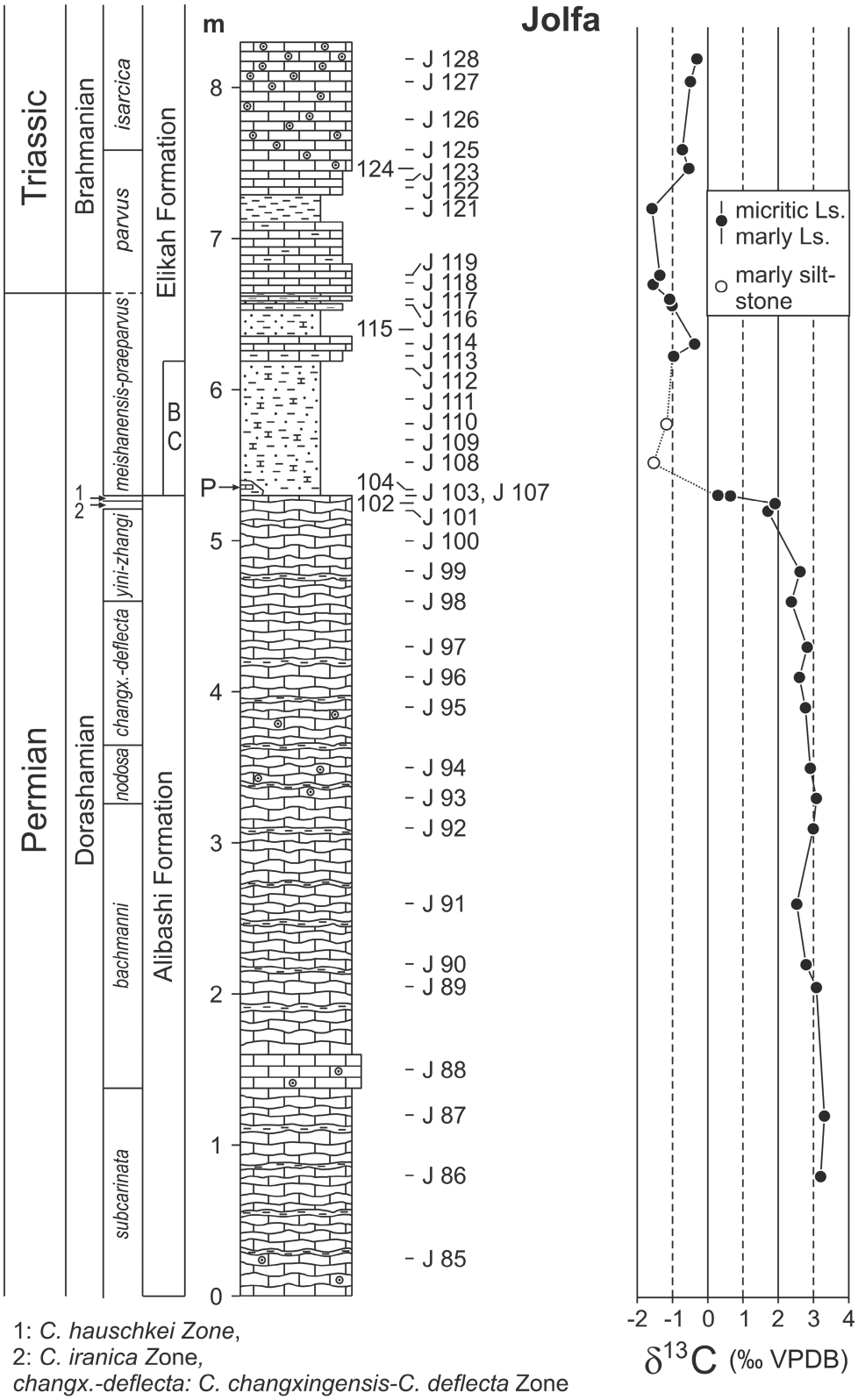

1: *C. hauschkei Zone*,
2: *C. iranica* Zone,
changx.-deflecta: C. changxingensis-C. deflecta Zone
BC: Boundary Clay
P: Small pockets of material washed out from unconsolidated rocks of the *C. hauschkei* and *C. iranica* Zones by a high energy event

explanations for Figs. 2, 3, 4, 5, 6

limestone
dolostone
nodular limestone
oolitic limestone
marly limestone
marl
clay, marly clay
silty marl, siltstone
crinoids

Fig. 2: Lithologic succession, biostratigraphy and $\delta^{13}C$ data of the Permian/Triassic boundary interval at Jolfa, NW-Iran (Kuh-e-Ali Bashi sections II-IV (Fig. 1) along the main arroyo). Two values (empty circles) were obtained from marly siltstones.

Years later, MEI SHILONG also re-studied Sweet's conodont collection from localities 1 and 4 sensu TEICHERT et al. (1973) and his results were published in SWEET & MEI (1999a, 1999b) (both authors did not visit or re-sample the Jolfa sections). From section 4 sensu TEICHERT et al. (1973) SWEET & MEI (1999a, 1999b) did not describe any Dorashamian conodonts, but only Dzhulfian (=Wuchiapingian) guide forms. These are, in ascending order: *C. dukouensis* MEI & WARDLAW, *C. asymmetrica* MEI & WARDLAW (junior synonym of *C. niuzhuangensis* LI ZHIHONG), *C. guangyuanensis* DAI & ZHANG: the holotype of this species is an advanced variety of *C. leveni* (KOZUR, MOSTLER & PJATAKOVA) and therefore a junior synonym of this species, *C. transcaucasica* (GULLO & KOZUR) and *C. orientalis* (BARSKOV & KOROLEVA). SWEET & MEI (1999a, 1999b) therefore rejected the Dorashamian age for the Alibashi Formation at locality 4 of TEICHERT et al. (1973). However, the re-sampling (by H.W.K.) of locality 4 (sensu TEICHERT et al. 1973) in 2002 confirmed the presence of Dorashamian conodonts in Sweet's material, as well as the presence of *Paratirolites* in a large part of the section, and other macrofaunas already mentioned in TEICHERT et al. (1973). Our two sampling campaigns (1998 and 2002) and the re-study of Sweet's conodont collection yield the following results: no species reported in SWEET & MEI (1999a, 1999b) from locality 4 is present in the Dorashamian and their locality 4 listed species, except for *C. transcaucasica* and *C. orientalis*, are not present even in the upper Dzhulfian to Dorashamian red pelagic beds of any other Iranian section. They are present only in the grey or black limestones, marls and shales. *C. dukouensis* has not yet been found in NW and Central Iran, because below the *C. niuzhuangensis* Zone no pelagic conodonts occur in shallow water facies. *C. niuzhuangensis* is present in the dark-grey to black upper *Codonofusiella* beds, far below the reddish Alibashi Formation at Jolfa locality 4. Even *C. orientalis*, the only species which occurs exclusively in the reddish pelagic upper Jolfa beds, is not present in the Dorashamian Alibashi Formation. MEI in SWEET & MEI (1999a, 1999b) likely misidentified *C. iranica* as *C. orientalis*, because they are morphologically similar, although they belong to different phylomorphogenetic lineages. *C. iranica* is common in all Iranian and Transcaucasian sections in the uppermost parts of the *Paratirolites* Limestone (except at the top of this unit) (KOZUR 2004). Considering that *C. orientalis* from the uppermost sample of section 4 in Sweet's collection is the guideform for the upper Dzulfian, the rest of this section was assigned to the middle and lower Dzhulfian.

Re-sampling (H.W.K.) in the upper *Paratirolites* Limestone at Jolfa locality 1 sensu TEICHERT et al. (1973) yielded, in ascending order, conodonts of the *C. changxingensis-C. deflecta, C. yini-H. praeparvus, C. iranica* and *C. hauschkei* Zones. The youngest sample of the *Paratirolites* Limestone in Sweet's conodont collection from section 1, the sample 20 U, taken at least 30 cm below its top, yielded conodonts of the *C. yini-C. zhangi* Zone, correctly assigned by SWEET & MEI (1999a, 1999b). From this section the level of the *C. iranica* and *C. hauschkei* zones was obviously not sampled by TEICHERT et al. (1973) because *C. iranica* is not present in Sweet's collection from section 1. SWEET & MEI (1999a, 1999b) could not have therefore misidentified *C. iranica* as *C. orientalis* at this locality and they correctly assigned it to the Dorashamian (Changxingian). The localities 1 and 4 of TEICHERT et al. (1973) are situated along the strike of the Alibashi Formation on the slope of a valley parallel to the Kuh-e-Ali Bashi main valley, and the beds can be easily traced in a nearly vegetation-free ~1 km long outcrop. These beds, that also have the same macrofauna, cannot be of Dorashamian age in section 1, and of lower to upper Dzhulfian age less than one km away, as assumed by SWEET & MEI (1999a, 1999b). SWEET & MEI (1999a, 1999b) attempted to confirm their conodont stratigraphy using a hypothetical fusulinid- and macrofauna succession at locality 4 and reported *Codonofusiella* in the lowermost part of the section. This fusulinid, however, cannot be present in the red pelagic facies of the Alibashi Formation, unless it was re-deposited together with other shallow water fossils, but such reworking is not present in the Jolfa region. This fusulinid genus is common in the shallow water dark-grey to black *Codonofusiella* beds below the Jolfa Formation s.s. At locality 4, *Araxilevis*, *Araxoceras* and *Vedioceras* were also reported by SWEET & MEI (1999a, 1999b) above *Codonofusiella*, but they are not present in the red-coloured Alibashi Formation at Jolfa or in any other Iranian section. The brachiopod *Araxilevis* is common in the dark-grey *Araxilevis* Beds of the lower Jolfa Formation, but it never occurs in the reddish Alibashi Formation and in the red upper Jolfa Formation. *Araxoceras* is also restricted to the grey lower Jolfa Formation. *Vedioceras* is present in the red upper Jolfa Formation (see also photograph of Fig. 7 in TEICHERT et al. 1973), but this is below the Alibashi Formation. Therefore, neither *Codonofusiella* nor the macrofaunas reported in SWEET & MEI (1999a, 1999b) can be present in the Alibashi Formation at Jolfa locality 4. It would not be possible to mistake the red-coloured Alibashi Formation of Jolfa locality 4 for the grey to black beds of the lower Dzhulfian from which all the above mentioned macrofaunas (except *Vedioceras*) and *Codonofusiella* are derived.

The present study is focussed on the Dorashamian to lowermost Triassic part of the succession in sections III and IV of our locality 1 (Fig. 1) that is on the slope of the Kuh-e-Ali Bashi main valley. The sequence begins with reddish hard nodular limestone with thin red marl and red shale intercalations of the upper Alibashi Formation comprising the upper *C. subcarinata*, *C. bachmanni*, *C. nodosa*, *C. changxingensis-C. deflecta*, *C. yini-C. zhangi*, *C. iranica and C. hauschkei* Zones (Fig. 2). In several adjacent sections the *Paratirolites* Limestone ends with a hardground (*Pleuronodoceras occidentale* ZAKHAROV and *Hypophiceras* sp. on its surface) that belongs, together with the underlying uppermost 2-5 cm of the *Paratirolites* Limestone, to the *C. hauschkei* Zone. In our sections III and IV (Figs. 1 and 2) the hardground is missing and a high-energy event at the base of the overlying Boundary Clay washed out parts of the not yet lithified uppermost *Paratirolites* Limestone (mostly the *C. hauschkei* Zone, partly the *C. iranica* Zone). The washed out conodonts were re-deposited in small, up to 14 cm thick, pockets of greenish-white clay and grey to pink limestone nodules with conodonts of the *C. iranica* and *C. hauschkei* Zones above the top of the *Paratirolites* Limestone (KOZUR 2004, and in

press). The overlying Boundary Clay consists of brown siltstone, marly siltstone and greenish-yellowish clay which contain the conodonts of the *C. meishanensis-H. praeparvus* Zone. As in Meishan (South China), *C. meishanensis* is only present in the lower part of this conodont zone. The Boundary Clay at Jolfa is overlain by mostly pinkish or yellowish, thin-bedded, platy or flaserbedded, marly limestones with intercalations of reddish brown, yellowish or greenish-grey to grey marly siltstones and shales. At the top of this unit an 18 cm thick marker horizon of grey shales with black layers is present within the lower *H. parvus* Zone of the lowermost Triassic. Above this marker horizon, are greyish-pinkish, brownish-violet weathered (except for their basal part) crinoid-bearing limestones of the upper *H. parvus* Zone and the *I. isarcica* Zone. For further information concerning the biostratigraphy of Late Permian to lowermost Triassic sediments at Jolfa see KOZUR (2004, and in press). In the Upper Dorashamian and lowermost Triassic beds in the Jolfa sections shallow water ostracods are absent, but kymatophobe ostracods, which avoid turbulent water movement, are common. The sediments were therefore deposited below the storm wave base. On the other hand, palaeopsychrosphaeric ostracods, which live in open sea environments at ~100 m water depths, but become common between 200 to 500 m (KOZUR 1991), are also absent. For these reasons, water depths between 60 and 80 m are assumed for the beds around the PTB in the Jolfa section. In the middle Dorashamian, below the *Paratirolites* limestone, *Acanthoscapha* and other palaeopsychrosphaeric ostracods are present suggesting that, at this level, the water depth was more than 100 m.

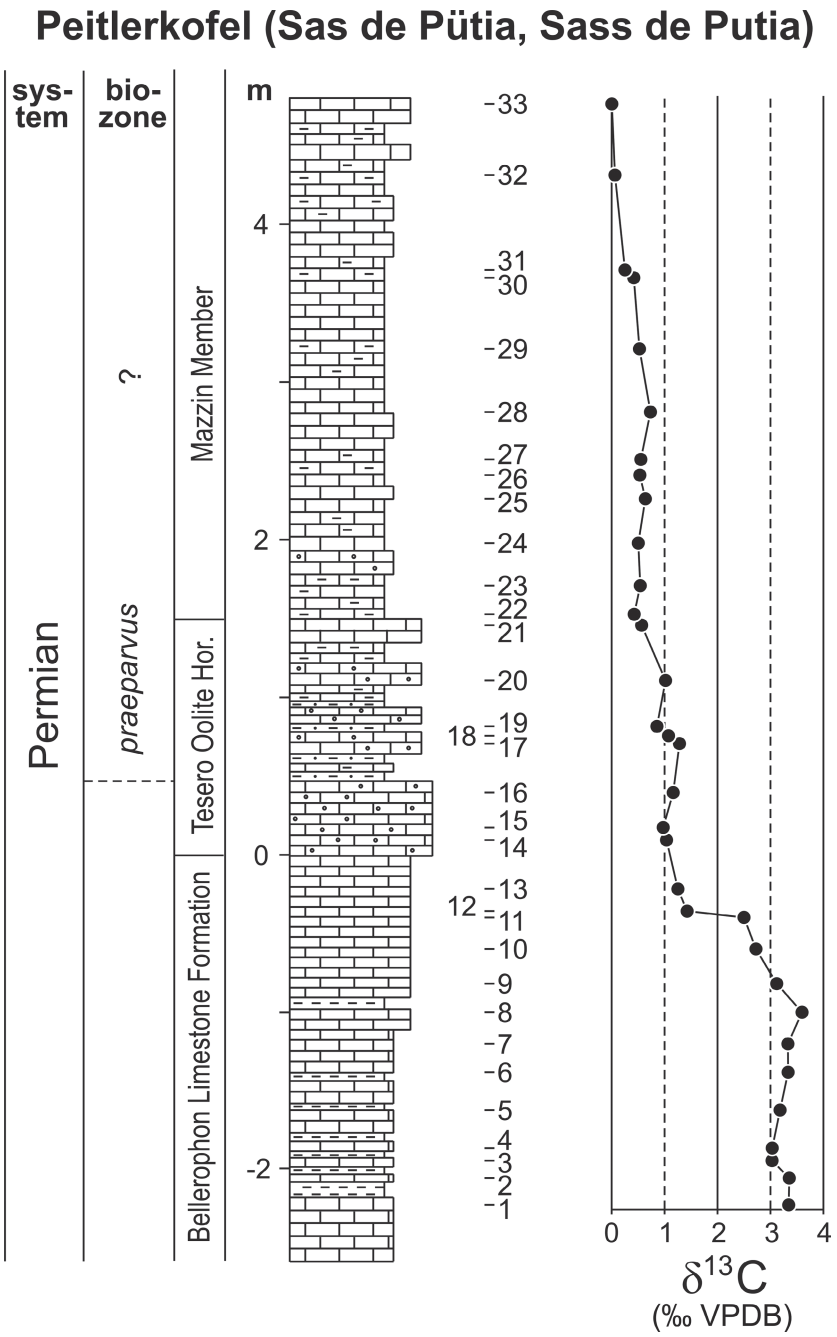

Fig. 3: Lithology and $\delta^{13}C$ record at the Peitlerkofel (Sas de Pütia, Sass de Putia) section in the Southern Alps (lithology slightly modified after BROGLIO LORIGA et al. 1986, see also NERI & POSENATO 1985); lithologic explanations in Fig. 2.

2.2. Southern Alps (Italy)

The uppermost Permian and the lowermost Triassic deposits of three South Alpine sections at Peitlerkofel (Sas de Pütia, Sass de Putia), Pufels (Bula, Bulla) and Tesero were investigated. Their lithologic sequences are similar. The uppermost part of the Late Permian Bellerophon Limestone Formation of the Southern Alps is overlain by oolitic limestones and marls of the Tesero Oolite Horizon (TOH), followed by the Mazzin Member (MM), both parts of the Werfen Formation. Traditionally (except KOZUR, 1994, who used the *H. parvus* boundary), the Permian-Triassic boundary is placed between the Bellerophon Limestone and the Werfen Beds at the base of the TOH. However, the International Commission on Stratigraphy defined the beginning of the Triassic with the FAD of *Hindeodus parvus* KOZUR & PJATAKOVA, which is found at a distinctly higher level in the Southern Alps. Conodonts are rare around the PTB in these sections and, consequently, the recognition of the PTB boundary is difficult.

2.2.1. Peitlerkofel (Sas de Pütia, Sass de Putia)

The Peitlerkofel (Sas de Pütia, Sass de Putia) section is described in BROGLIO LORIGA et al. (1986) and illustrated in Figure 3 (see also KOZUR 1994, NERI & POSENATO 1985). The uppermost part of the Bellerophon Limestone Formation is rich in fossils (foraminifers, algae, crinoids, echinoid remains, brachiopods). The overlaying TOH is 1.5 m thick and contains Permian fauna (BROGLIO LORIGA et al. 1986, KOZUR 1994). The still higher MM of the Werfen Formation includes marly mudstone and limestone (partly oolitic). *H. praeparvus* KOZUR and *Stepanovites dobruskinae* KOZUR & MOVSHOVICH were found throughout the TOH, except in the lowermost 0.5 m (KOZUR unpublished). Consequently, in this section the Triassic begins above the TOH. The MM was not investigated for conodonts and hence the FAD of *H. parvus*, and with it the base of the Triassic, has not been biostratigraphically localised (Fig. 3).

2.2.2. Pufels (Bula, Bulla)

The uppermost Bellerophon Formation of the Pufels section (Fig. 4) consists of dark-grey limestones and black silty marls (see MOSTLER 1982). The limestones are rich in fossils and contain brachiopods, gastropods, algae, bivalves, foraminifers, bryozoans, ostracods, ophiurians and echinoids. The overlaying 6 m-thick TOH varies between oolitic limestones (poor in fossils) and micritic limestones beds. In the succeeding MM marls and limestones with bivalves and ostracods were deposited.

In the Pufels area, conodonts were studied by HUCKRIEDE (1958) and STAESCHE (1964), and KOZUR & MOSTLER (in MOSTLER 1982) subdivided the section using the conodonts. This biostratigraphy was refined by PERRI (1991) and FARABEGOLI & PERRI (1998). The *H. praeparvus*, *H. parvus* and *I. isarcica* Zones are present in the sequence. The lithology and sample numbers in this study (Fig. 4) are taken from PERRI (1991) and FARABEGOLI & PERRI (1998), with some new numbers added. The conodont zonation is slightly modified. According to PERRI (1991) and FARABEGOLI & PERRI (1998), the FAD of *H. parvus* is within the sample BU 12B from the middle TOH. However, FARABEGOLI & PERRI (1998) illustrated from this sample a juvenile *H. praeparvus* with a rather large cusp. Note that juvenile *Hindeodus* are difficult to determine and in times of extraordinary ecological stress around the PTB, the intraspecific variability in *H. praeparvus* is very high. Very rarely, forms with large but broad cusps are present that have some similarity to *H. parvus*. One such specimen was found in Bed 25 of Meishan and originally assigned to *H. parvus*, but later (e.g. YIN & ZHANG 1996) to *H. latidentatus* (KOZUR, MOSTLER & RAHIMI-YAZD). KRYSTYN (pers. comm. to Kozur) found such a specimen also at Abadeh, below the base of the *H. parvus* Zone and KOZUR found several of these specimens below the base of the Triassic and at the base of the *H. parvus* Zone in the Zal section (NW-Iran). These rare disaster forms that belong to a new species (KOZUR 2004). From the middle TOH at Pufels (sample BU 13B), FARABEGOLI & PERRI (1998) illustrated a *Hindeodus* as *H. parvus*. However, the posterior end of this specimen is somewhat thickened and rounded, as in *Hindeodus eurypyge* (NICOLL, METCALFE & WANG). This species occurs in both the *H. praeparvus* and in the *H. parvus* Zone. Wide, chisel-like denticles occur in this species only in mature specimens, whereas juvenile and late juvenile specimens have pointed or needle-like denticles. As only one specimen is present in sample BU 13B, it cannot be resolved whether it is a late juvenile *H. eurypyge* or a *H. parvus*. In both cases the *H. parvus* Zone begins much later than assumed by FARABEGOLI & PERRI (1998).

2.2.3. Tesero

The uppermost Bellerophon Formation of the PTB section in Tesero (Fig. 5) consists of dolostones and bioclastic (algae, foraminifers, echinids, etc.) carbonates. In the succeeding TOH carbonates with bivalves, foraminifers and gastropods alternate with oolitic limestone. The overlaying MM consists of marly limestones and mudstones with thin biocalcarenite storm layers. For further information see NERI (1999).

Conodont investigations have been made by ASSERETO et al. (1973), PERRI (1991), NICORA & PERRI (1999) and KOZUR (unpublished data) and their zonations are used in this study. Carbon isotope values have previously been determined using whole rock carbonates from this locality by MAGARITZ et al. (1988) and their database has been enlarged in this work (Fig. 5).

2.3. Gerennavár (Hungary)

The marine sediments of the PTB section at Gerennavár (Bükk Mts., Hungary) begins with the Late Permian dark limestones of the Nagyvisnyó Formation (equivalent of the Badiota facies of the Bellerophon Limestone), overlain by the Boundary Clay, and followed by thin-bedded micritic, marly limestones of the Gerennavár Limestone Formation (equivalent of the MM) (Fig. 6). The water depth during

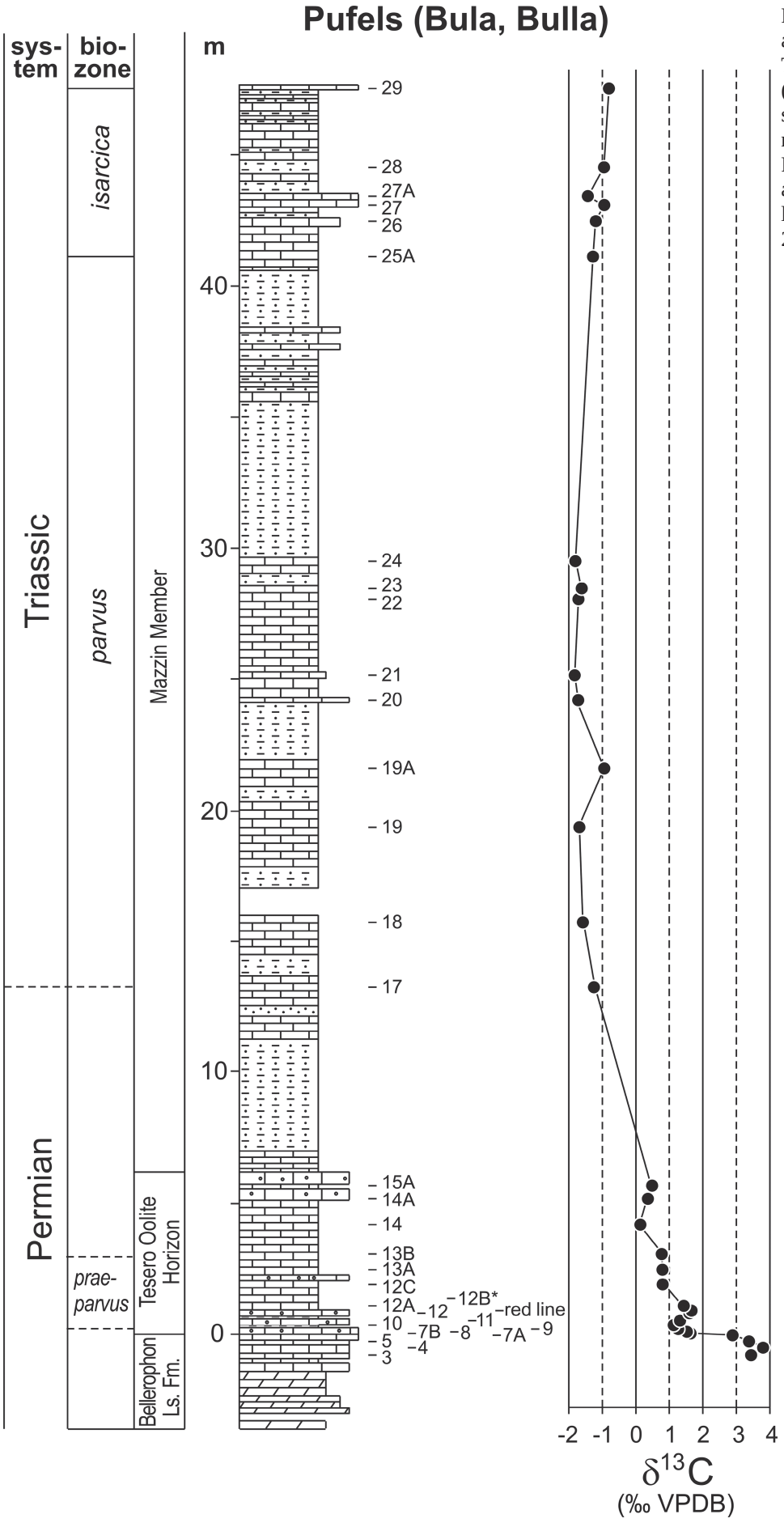

Fig. 4: Carbon isotope values and lithology at the Permian/Triassic boundary at Pufels (lithology, biostratigraphy and sample numbers slightly modified after PERRI (1991) and FARABEGOLI & PERRI (1998); see also SCHOLGER et al. (2000); lithologic explanations in Fig. 2.

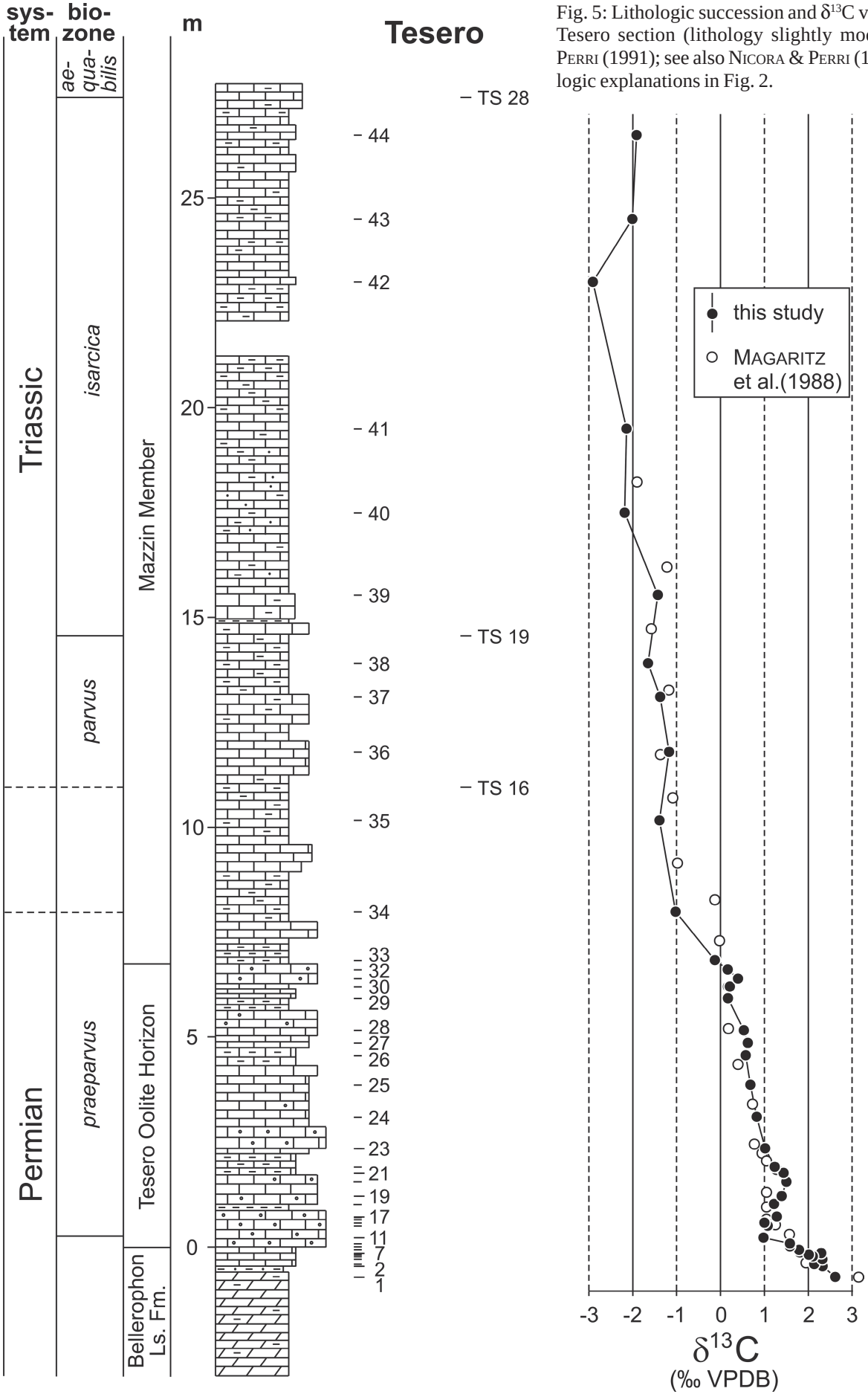

Fig. 5: Lithologic succession and $\delta^{13}C$ values of the Tesero section (lithology slightly modified after PERRI (1991); see also NICORA & PERRI (1999); lithologic explanations in Fig. 2.

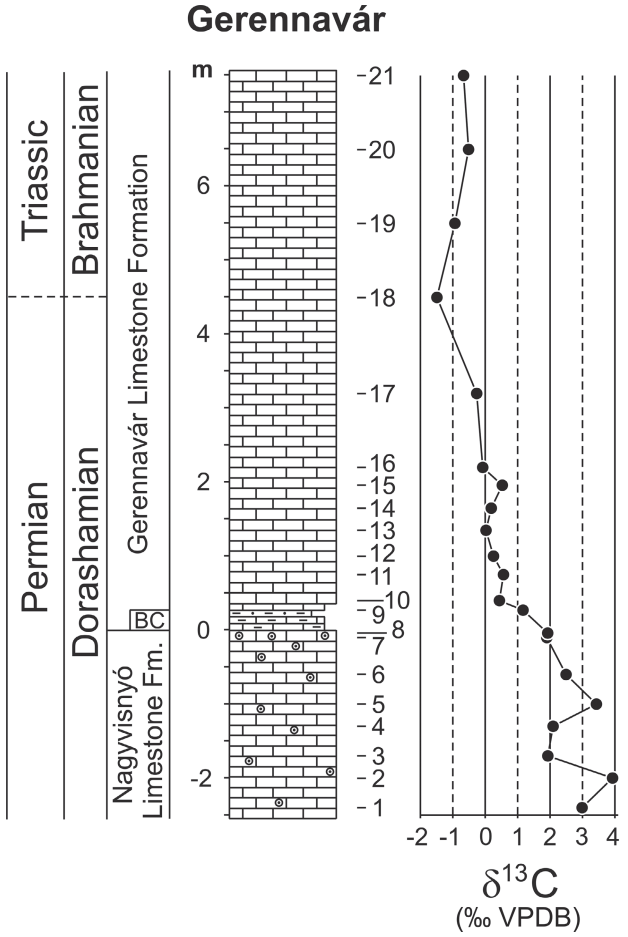

Fig. 6: PTB section at Gerennavár (Bükk Mts., Hungary) with lithology and carbon isotope record; lithologic explanations in Fig. 2; BC: Boundary Clay.

deposition was deeper than in the Southern Alps, as attested by the preservation of the Boundary Clay, which contains clastic components that are absent in the sediments below and above (KOZUR 1988). In addition, cosmic microsphaerules are present (DETRE et al. 2002). The higher water depth during the deposition of the upper Nagyvisnyó Formation, compared with the upper Bellerophon Limestone Formation of the Southern Alps, is indicated by the composition of the ostracod fauna, comprising only stenohaline marine forms in the upper Nagyvisnyó Formation, among them some spined forms (KOZUR 1985) which do not occur in the upper Bellerophon Formation of the Southern Alps. Moreover, there is a common presence of conodonts in the upper Nagyvisnyó Formation (KOZUR & MOCK 1977), whereas conodonts are missing or extremely rare in the upper Bellerophon Limestone Formation of the Southern Alps because of the very shallow water depth.

3. Methods

For the $\delta^{13}C$ analyses only homogeneous rock material – mostly micritic limestones and mudstones – was used, weathered portions or veins were rejected. Between 0.15 to 0.45 mg carbonate powder was drilled from a fresh surface and reacted with 5-7 drops of H_3PO_4 in a borosilicate exetainer after flushing with helium and heating to 72.0 ± 0.1°C. The generated CO_2 was separated from water vapor and their carbon and oxygen isotope values (Tab. 1) were measured using a ThermoFinnigan GasBench II linked to a Delta^{plus}XL mass spectrometer (SPÖTL & VENNEMANN 2003). The external precision, calculated over 12 standards per batch, was typically 0.05-0.06 ‰ for $\delta^{13}C$ and 0.06-0.08 ‰ for $\delta^{18}O$. Results were calibrated against the V-PDB standard.

4. Results and Discussion

Owing to the deposition in an open marine environment at depths in excess of 60 meters and the presence of all conodont zones (CAI = 1), the investigated Jolfa succession provides a good section for an inorganic carbon isotope curve (Fig. 2, Tab. 1). The $\delta^{13}C$ values vary around 3 ‰ in the *C. subcarinata* and *C. bachmanni* Zones, except for one $\delta^{13}C$ value around 2.5 ‰ in the middle *C. bachmanni* Zone. The continuous decrease begins in the upper *C. nodosa* Zone and continues in the *C. changxingensis-C. deflecta*, *C. yini-C. zhangi*, *C. iranica* Zones, reaching values between 0.6 and 0.3 ‰ in the *C. hauschkei* Zone. The change from the *C. hauschkei* Zone to the *C. meishanensis-H. praeparvus* Zone is accompanied by a change from carbonate (biomicritic limestone) into clastic (siltstone, shale) dominance and by disappearance of all stenotherm warm water faunal elements. Two samples of the lower *C. meishanensis-H. praeparvus* Zone are marly siltstones (J 108 and J 110; Fig. 2; empty circles) and their $\delta^{13}C$ values are low at around -1.5 ‰. A short increase of carbon isotope values in the middle of the *C. meishanensis-H. praeparvus* Zone is followed by a decrease to -1.6 ‰ in the lowermost Triassic *H. parvus* (J 118) and a subsequent increase to the *I. isarcica* Zone by more than 1 ‰.

The general carbon isotope trend from ~ 3 ‰ in the Dorashamian to negative values in the lowermost Triassic for the Kuh-e-Ali Bashi section at Jolfa was previously reported by HOLSER & MAGARITZ (1987), BAUD et al. (1989) and MAGARITZ (1989) for whole rock carbonates, but the biozones were not given and – particularly above the Boundary Clay in the topmost Permian and lowermost Triassic – only a few data points were presented. It is difficult to integrate these published data into our dataset that is based on a highly resolved biostratigraphic subdivision. The literature-data are therefore not shown in Figure 2.

The Jolfa carbon isotope curve is important for comparison with other PTB sections because of its good biostratigraphic background and because the micritic samples were deposited in an open marine oxic environment. Between samples J 99 and J 101 and J 102 und J 107, a decrease in $\delta^{13}C$ of 0.91 and 1.27 ‰, respectively is accompanied by a decrease in $\delta^{18}O$ of 1.34 and 1.32 ‰, respectively (Tab. 1). Therefore it cannot be entirely excluded that alteration may have overprinted the primary isotope trend for these two levels although these isotope values originate from micritic

Jolfa

no.	m	$\delta^{13}C$	$\delta^{18}O$
J 86	0.80	3.20	-5.56
J 87	1.20	3.31	-3.87
J 89	2.05	3.08	-5.04
J 90	2.20	2.79	-5.15
J 91	2.60	2.52	-5.59
J 92	3.10	2.99	-5.07
J 93	3.30	3.08	-4.91
J 94	3.50	2.91	-5.11
J 95	3.90	2.77	-4.77
J 96	4.10	2.60	-4.93
J 97	4.30	2.82	-4.85
J 98	4.60	2.37	-5.55
J 99	4.80	2.62	-4.95
J 101	5.20	1.71	-6.29
J 102	5.25	1.91	-5.67
J 107	5.30	0.64	-6.99
J 103	5.31	0.29	-6.12
J 108	5.52	-1.53	-6.75
J 110	5.78	-1.17	-6.90
J 113	6.23	-0.97	-6.71
J 114	6.31	-0.37	-6.48
J 116	6.56	-1.01	-6.85
J 117	6.60	-1.08	-6.81
J 118	6.70	-1.55	-6.90
J 119	6.76	-1.36	-7.02
J 121	7.20	-1.58	-6.93
J 124	7.47	-0.53	-6.28
J 125	7.59	-0.72	-6.70
J 127	8.04	-0.49	-6.82
J 128	8.19	-0.31	-6.25

Peitlerkofel
(Sas de Pütia, Sass de Putia)

no.	m	$\delta^{13}C$	$\delta^{18}O$
1	-2.22	3.34	-5.04
2	-2.05	3.36	-5.18
3	-1.94	3.03	-5.31
4	-1.86	3.03	-5.27
5	-1.62	3.18	-3.87
6	-1.40	3.33	-5.23
7	-1.20	3.33	-7.52
8	-1.00	3.59	-5.50
9	-0.82	3.12	-6.54
10	-0.60	2.72	-7.93
11	-0.40	2.50	-6.44
12	-0.36	1.42	-7.02
13	-0.22	1.25	-6.40
14	0.09	1.04	-5.96
15	0.17	0.97	-5.31
16	0.39	1.16	-5.58
17	0.70	1.28	-6.97
18	0.75	1.08	-6.64
19	0.81	0.86	-6.90
20	1.10	1.02	-6.62
21	1.48	0.57	-7.17
22	1.52	0.43	-7.37
23	1.70	0.54	-7.21
24	1.97	0.50	-7.27
25	2.25	0.64	-6.53
26	2.40	0.54	-7.26
27	2.50	0.55	-6.95
28	2.80	0.73	-6.22
29	3.20	0.53	-6.34
30	3.65	0.42	-6.34
31	3.70	0.25	-7.98
32	4.30	0.06	-6.87
33	4.75	0.00	-7.46

Pufels
(Bula, Bulla)

no.	m	$\delta^{13}C$	$\delta^{18}O$
BU 03	-0.80	3.44	-5.69
BU 04	-0.52	3.80	-5.51
BU 05	-0.28	3.38	-6.28
BU 07 A	-0.04	2.88	-6.24
BU 07 B	0.03	1.63	-8.11
BU 08	0.09	1.52	-8.34
BU 09	0.20	1.26	-7.90
BU 10	0.35	1.13	-6.86
BU 11	0.52	1.32	-6.89
BU 12	0.80	1.60	-5.68
BU red line	0.90	1.66	-6.14
BU 12 A	1.08	1.43	-6.69
BU 12 C	1.91	0.80	-7.19
BU 13 A	2.47	0.79	-6.63
BU 13 B	3.07	0.77	-6.82
BU 14	4.20	0.13	-6.53
BU 14 A	5.19	0.36	-7.50
BU 15 A	5.69	0.49	-7.18
BU 17	13.30	-1.25	-6.08
BU 18	15.79	-1.58	-6.15
BU 19	19.43	-1.68	-6.44
BU 19 A	21.69	-0.94	-6.74
BU 20	24.30	-1.72	-7.04
BU 21	25.26	-1.82	-6.35
BU 22	28.17	-1.71	-6.27
BU 23	28.59	-1.61	-6.60
BU 24	29.63	-1.80	-6.49
BU 25 A	41.31	-1.28	-7.19
BU 26	42.66	-1.19	-6.79
BU 27	43.28	-0.95	-7.17
BU 27 A	43.62	-1.43	-6.68
BU 28	44.72	-0.95	-6.54
BU 29	47.75	-0.80	-6.84

for Peitlerkofel, Pufels and Tesero:
0 cm = boundary between
Bellerophon Ls. Fm. and Tesero
Oolite Horizon

Tesero

no.	Tes	m	$\delta^{13}C$	$\delta^{18}O$
1	Tes 46	-0.72	2.61	-1.69
2	Tes 49 B	-0.46	2.33	-5.08
3	Tes 50	-0.41	2.14	-5.33
4	Tes 51	-0.29	2.32	-5.67
5	Tes 52	-0.23	2.10	-5.57
6	Tes 53	-0.19	2.01	-4.77
7	Tes 54	-0.15	2.29	-5.65
8	Tes 56	-0.07	1.79	-6.11
9	Tes 58	0.01	1.58	-6.03
10	Tes 59	0.08	1.58	-6.52
11	Tes 61	0.22	0.98	-6.46
12	Tes 63	0.50	1.08	-6.07
13	Tes 64	0.58	1.00	-5.94
14	Tes 64	0.58	1.22	-5.76
15	Tes 65	0.65	1.21	-6.02
16	Tes 66	0.71	1.28	-6.47
17	Tes 67	0.72	1.28	-6.59
18	Tes 70	1.03	1.22	-6.64
19	Tes 71	1.22	1.40	-6.24
20	Tes 72	1.55	1.50	-6.12
21	Tes 73	1.77	1.44	-6.16
22	Tes 74	1.91	1.23	-6.36
23	Tes 77	2.35	1.02	-6.23
24	Tes 77 A	3.10	0.82	-6.89
25	Tes 77 B	3.86	0.68	-6.58
26	Tes 77 C	4.56	0.57	-5.85
27	Tes 77 D	4.86	0.62	-6.27
28	Tes 84	5.16	0.53	-6.28
29	Tes 87	5.92	0.17	-5.72
30	Tes 88	6.21	0.17	-5.78
31	Tes 89	6.40	0.40	-5.96
32	Tes 89 B	6.61	0.16	-6.27
33	Tes 91	6.83	-0.13	-5.17
34	Tes 94	7.99	-1.03	-5.41
35	Tes 97	10.17	-1.39	-5.80
36	Tes 98	11.80	-1.17	-6.20
37	Tes 99 A	13.11	-1.38	-5.97
38	Tes 99 AB	13.91	-1.65	-5.73
39	Tes 99 D	15.54	-1.43	-5.90
40		17.50	-2.19	-5.64
41		19.50	-2.14	-5.64
42		23.00	-2.91	-5.70
43		24.50	-2.01	-5.58
44		26.50	-1.91	-5.52

Gerennavár

no.	m	$\delta^{13}C$	$\delta^{18}O$
1	-2.40	2.99	-6.36
2	-2.00	3.93	-7.24
3	-1.70	1.93	-7.04
4	-1.30	2.09	-7.92
5	-1.00	3.43	-7.04
6	-0.60	2.50	-7.28
7	-0.10	1.90	-7.19
8	-0.04	1.93	-7.21
9	0.27	1.17	-7.26
10	0.40	0.44	-7.18
11	0.75	0.56	-7.42
12	1.00	0.26	-7.46
13	1.35	0.02	-7.50
14	1.65	0.19	-7.71
15	1.96	0.53	-7.43
16	2.20	-0.08	-7.67
17	3.20	-0.26	-7.71
18	4.50	-1.49	-7.71
19	5.50	-0.94	-7.55
20	6.50	-0.52	-7.42
21	7.50	-0.67	-7.56

for Gerennavár: 0 cm =
boundary between
Nagyvisnyó Formation and
Boundary Clay

Tab. 1: Carbon and oxygen isotope data (samples „Tes“ from NICORA & PERRI 1999)

limestones and may present, at least for carbon, the nearly primary isotope signal of ancient seawater. Only the two $\delta^{13}C$ values of the slightly marly siltstones (J 108 and J 110; Fig. 2) from the Boundary Clay (~ -1.5 ‰) must be regarded with caution because of their partially clastic lithology; these samples are more prone to diagenetic overprint. In the same biostratigraphic level (lower *C. meishanensis-H. praeparvus* Zone) of other pelagic Iranian sections at Shahreza and Zal, the $\delta^{13}C$ values of the nearly unweathered Boundary Clays are between 2.1 ‰ and 1.3 ‰ (KORTE et al. 2004b) and 1.1 ‰ and 0.7 ‰ (KORTE et al. 2004c), respectively. This is similar to shallow water sections of the Alps that lack the Boundary Clay facies (Figs. 3, 4 and 5; see also HOLSER et al. 1989, NEWTON et al. 2004). For Jolfa (and for Abadeh, see KORTE et al. 2004a) the negative values of the (lower) Boundary Clay were obtained from shales and siltstones with low carbonate contents, and their carbon isotope signal may have been altered during modern-day weathering. This also may have been the case for the strongly weathered Boundary Clay at the Meishan PTB-section (see also BOWRING et al. 1998) from which low carbon isotope values up to –5 ‰ were reported by XU & YAN (1993) and JIN et al. (2000). The negative carbon isotope values for the lower *C. meishanensis-H. praeparvus* Zone (Boundary Clay) at Jolfa and some other pelagic PTB sections is thus probably a result of post-depositional alteration (see also KORTE et al. 2004b).

The middle *C. meishanensis-H. praeparvus* Zone at Jolfa, in which the carbonate facies is again pronounced, is characterised by a slight short ~ 0.6 ‰ rise in $\delta^{13}C$, similar to other pelagic sections with a high resolution carbon isotope record (KORTE et al. 2004b, 2004c). With the exception of the data reported by JIN et al. (2000) for the Meishan section, in any complete pelagic and shallow water PTB sections a $\delta^{13}C$ minimum occurs around the PTB (e.g. BAUD et al. 1989, HOLSER et al. 1989, NEWTON et al. 2004, KORTE et al. 2004a, 2004b, 2004c). At Jolfa the lowest trustworthy carbon isotope value has also been observed at the base of the Triassic (Fig. 2), in the lower *H. parvus* Zone (–1.55 ‰). This general feature enables the utilisation of the carbon isotope values as a stratigraphic tool for location of the PTB. A second distinct $\delta^{13}C$ minimum in the lower *I. isarcica* Zone has been reported for a shallow water section at the Gartnerkofel core in the Carnic Alps (HOLSER et al. 1989) and for pelagic sediments at Shahreza (KORTE et al. 2004b), but has not been observed in the Jolfa section.

The PTB in the Southern Alps lies in typical shallow water deposits. The uppermost Bellerophon Limestone is very rich in green algae, typical shallow water ostracods (e.g. *Hollinella*, Kirkbyacea) and other shallow water fossils. Lithofacies, lithology and microfacies of the TOH also indicate very shallow water conditions (e.g. oolitic limestone, storm layers). Pelagic conodonts (gondolellids) are absent in both the Bellerophon Limestone and the TOH, but typical shallow water conodonts are present in the TOH and in the overlying MM (*Hindeodus*, *Isarcicella*, *Stepanovites*). The faunas indicate water depths shallower than 20 m for the uppermost Bellerophon Limestone Formation and the TOH. However, the occurrence of marine faunas indicates continuous marine conditions in the investigated sections of the Southern Alps (Peitlerkofel, Pufels, Tesero) and at least no biostratigraphic gap was recognised. These observations and the fact that the Late Permian decline of the carbon isotopes is - in timing and magnitude - similar to those of open marine sections (e.g. BAUD et al. 1989, HOLSER et al. 1989, NEWTON et al. 2004, KORTE et al. 2004a, 2004b, 2004c) indicate that the $\delta^{13}C$ values of the investigated carbonate rocks of the Southern Alps can be regarded as nearly a primary signal of ancient seawater.

In order to compare the three investigated Southern Alps sections chemostratigraphically with each other and with other successions of the same region and with the Gerennavár section, their carbon isotope curves have been correlated in Figure 7 by using the ~ 2.0 ‰ and the ~ 0 ‰ chemostratigraphic levels. At Peitlerkofel the 2 ‰ level (a sudden decrease of the $\delta^{13}C$ values from 2.5 to 1.3 ‰) lies about 0.4 m below the top of the Bellerophon Limestone and in Gerennavár 0.2 m below the top of the Nagyvisnyó Formation (equivalent of the Badiota facies of the Bellerophon Formation). On the other hand, at Tesero and Pufels the 2 ‰ level lies at the base of the TOH (sudden drops occur from 2.5 to 1 ‰ and 3 to 1.5 ‰, respectively). In these two sections the carbon isotope values in the uppermost Bellerophon Formation are more than 1 ‰ higher than in the Peitlerkofel section. The $\delta^{13}C$ decline continues in the South Alpine PTB sections, reaching 0 ‰ close to the top of the TOH in the Tesero section (no carbon isotope values are available for the Pufels section), but >3 m above the top of the TOH in the MM of the Peitlerkofel section (Fig. 7).

Carbon isotope values of whole rock carbonates have been published for the Seis (Siusi) section by NEWTON et al. (2004) and for the San Antonio section (Carnic Alps) by BRANDNER (1988) and OBERHÄNSLI et al. (1989) (Fig. 7). For the Seis section only a few $\delta^{13}C$ values exist and a comparison to Tesero, Pufels and Peitlerkofel is difficult, but it seems that the 2 ‰ chemostratigraphic level is within the TOH, and therefore the oolite facies started at Seis earlier than in all other discussed South Alpine sections.This is consistent with the palaeomagnetic data from SCHOLGER et al. 2000). Additionally, the 0 ‰ chemostratigraphic level of this locality is within the upper TOH, indicating that the oolite facies lasted longer than in the more eastern sections.

The $\delta^{13}C$ values of the PTB-sections of the Southern Alps indicate that the lithologic changes from the Bellerophon Formation to the TOH (the previous Permian/Triassic boundary in the Southern Alps) and from the TOH to the MM are slightly diachronous. This was generally accepted for the TOH/MM contact since ASSERETO et al. (1973) (e.g. WIGNALL & HALLAM 1992), but the boundary between the Bellerophon Limestone and TOH was, up to recent time, regarded as an isochronous boundary s.s. (SCHOLGER et al. 2000).

Our results back up KOZUR (1994) but contradict the statement of SCHOLGER et al. (2000: 504) that „the current event (i.e. boundary event) at the base of the Tesero Horizon can be regarded as synchronous boundary in a strict sense“. This statement is based on their palaeomagnetic data, which in fact show that the Bellerophon Limestone–Tesero Oolite and the TOH-MM boundaries have diachronous character. Note that the diachronous character of the latter boundary was recognised also by SCHOLGER et al. (2000). In

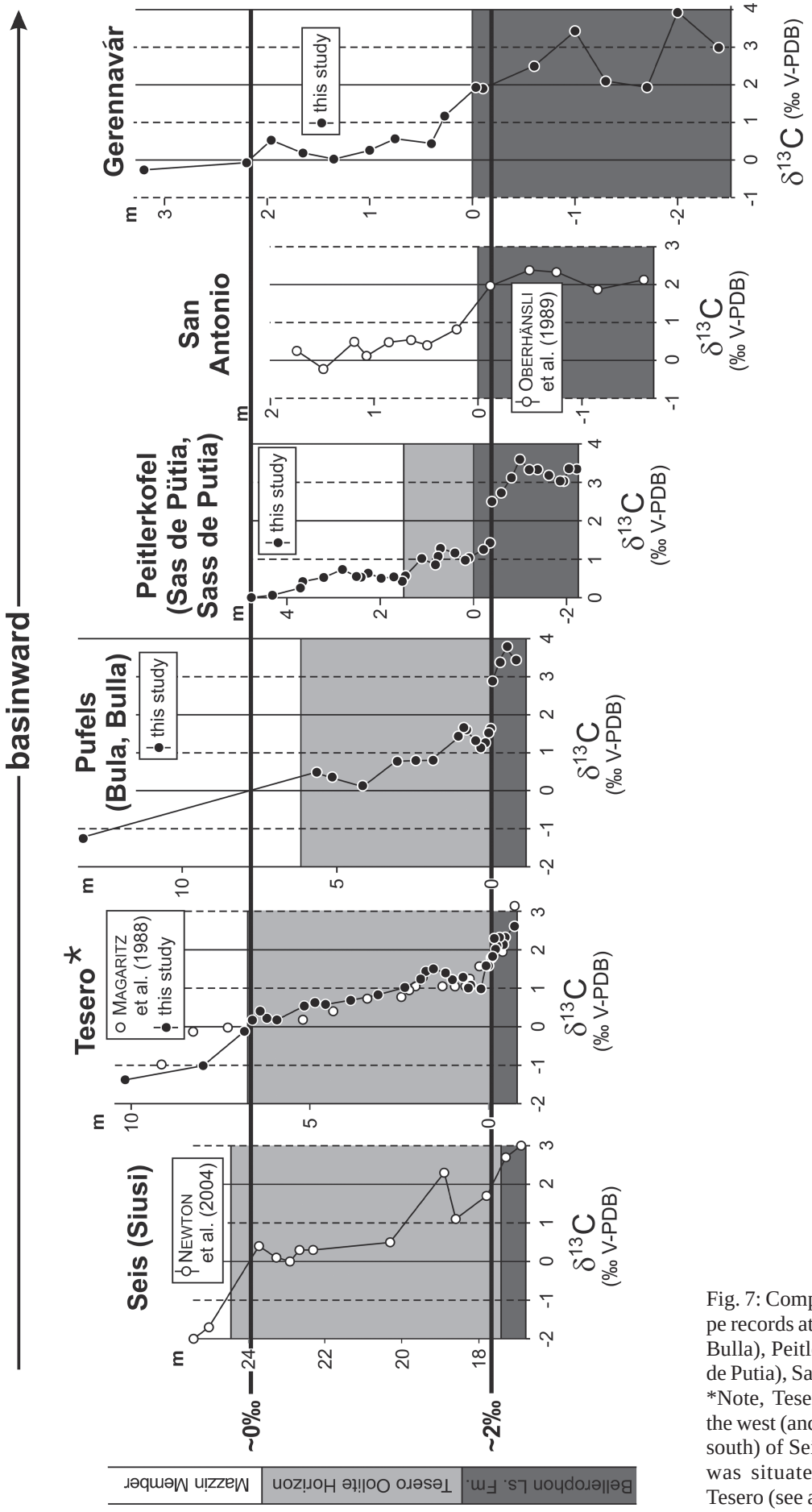

Fig. 7: Comparison of the carbon isotope records at Seis, Tesero, Pufels (Bula, Bulla), Peitlerkofel (Sas de Pütia, Sass de Putia), San Antonio and Gerennavár. *Note, Tesero is somewhat further to the west (and about 30 km further to the south) of Seis, but the former coastline was situated closer to Seis than to Tesero (see also BRANDNER 1988).

the Pufels (Bula, Bulla) section, the last reversed sample was 5 cm below, the first normally magnetised sample 5 cm above, the top of the Bellerophon Limestone, the reversal is thus practically at the very base of the Werfen Beds. In the Seis (Siusi) section, the last sample with reversed polarity is within the upper TOH, 42 cm above the top of the Bellerophon Limestone, and the first sample with normal magnetisation is 72 cm above the top of the Bellerophon Limestone. Thus at Pufels the Bellerophon Limestone/ Tesero Oolite boundary is stratigraphically higher than in the Seis section. There it can be equivalent to the top of the TOH sensu SCHOLGER et al. (2000) or be even higher, within the lowermost MM. Note that, compared to SCHOLGER et al. (2000), NEWTON et al. (2004) assumed that the upper boundary of the TOH is much higher up in the Seis section, but these discrepancies do not influence the fact that at least the bottom 42 cm of the TOH at Seis correspond to the uppermost Bellerophon Limestone at Pufels.

The diachronous characters of both boundaries (Bellerophon Limestone to TOH and TOH to MM) – also assumed from evaluation of the faunal distributions in the Dolomites by KOZUR (1994) – can have the following explanation. The change from the Badiota facies of the Bellerophon Limestone to the TOH indicates a regression caused by a slight sea-level drop. The facies change from the TOH to the MM was caused by a subsequent slight sea level rise. The Pufels section was situated east (NE) of Tesero and west of the Peitlerkofel. The Seis (Siusi) section was situated west of Pufels, but east of Tesero. Note, the former coastline was situated closer to Seis than to Tesero because the last was situated about 30 km further in the south (see also BRANDNER 1988). Based on the $\delta^{13}C$ values, the TOH begins earlier in the west, where the water depth was generally shallower (see also ASSERETO et al. 1973, BRANDNER 1988). At the time of sea level rise, the TOH was replaced by the MM, this time earlier in the east. In the Comelico area of the eastern Southern Alps, the TOH finally disappears and the MM lies directly on the Bellerophon Limestone (see NOÉ 1987; BRANDNER 1988). The lower TOH of the western Dolomites is an equivalent of the uppermost Bellerophon Limestone further in the east, and the middle and upper TOH is replaced by the MM. Finally, the Tesero Oolite facies disappeared in the east because the water depth remained too deep for forming the oolitic limestones. This is also the case for the San Antonio section (east of Peitlerkofel), where no Tesero Oolite facies exist (see OBERHÄNSLI et al. 1989). Any comparison of the carbon isotope values of this locality with those of other successions is difficult. In the last 1.7 m of the Bellerophon Limestone at the San Antonio section a slight increase, from 2 to 2.4 ‰, and a decline, from 2.4 to 2 ‰, is followed by a decline to 0.4 ‰ after the facies change into the MM. More data are needed for a more precise $\delta^{13}C$-curve, but the best interpretation for San Antonio chemostratigraphic results is that the lower TOH of the western Dolomites – similar to Peitlerkofel – is replaced by the uppermost Bellerophon Limestone whereas the middle and upper TOH is replaced by the facies of the MM (Fig. 7). Towards the basin centre (in the east) the Bellerophon Limestone Formation does not terminate by shallowing-induced replacement of this formation by the Tesero Oolite facies, but the fossil-rich Badiota facies of the Bellerophon Limestone Formation (or of the contemporaneous Nagyvisnyó Formation of the Bükk Mountains) changes abruptly into the Mazzin facies which is very poor in fossils. This can be observed at Gerennávar (Bükk Mountains, Hungary) where the Tesero Oolite facies is absent and the Nagyvisnyó Formation is directly overlain by thin marly siltstones and marls of the Boundary Clay followed by thin-bedded, marly limestones of the lower Gerennavár Limestone Formation (equivalent of the Mazzin Member) (Figs. 6 and 7). The mass extinction at the base of the Boundary Clay at the Gerennavár section allows the correlation with the event boundary of the pelagic PTB sections in Iran and China. The carbon isotope values of the Gerennavár section decline from > 3 to ~ 1.9 ‰ within the uppermost Nagyvisnyó Formation, and the decline continues within the lowermost Gerennavár Formation towards ~ -1.5 ‰ at the base of the Triassic. This carbon isotope trend is similar to that of the San Antonio section (Carnic Alps), indicating that the very base of the MM in these sections corresponds to the middle and upper TOH of the western Dolomites.

5. Conclusions

Late Dorashamian and basal Triassic beds in the Jolfa section (Iran) were deposited in water depths in excess of 60 meters. All pelagic conodont zones are present in this locality. The carbon isotope record in the Jolfa section varies around 3 ‰ (V-PDB) in the *C. subcarinata* and *C. bachmanni* Zones, decreases from the *C. nodosa* Zone, reaches -1.55 ‰ in the *H. parvus* Zone and increases again to -0.5 ‰ in the *I. isarcica* Zone. The $\delta^{13}C$ curve of the Jolfa section is similar to other open marine pelagic sections. The patterns of the $\delta^{13}C$ drop in the upper Permian and the presence of all established conodont zones suggest that the entire Dorashamian sedimentary sequence exists in this locality.

The $\delta^{13}C$ values of the three South Alpine sections, Peitlerkofel, Pufels and Tesero, indicate that the lithologic changes from the Bellerophon Formation to the TOH, the previous Permian/Triassic boundary in the Southern Alps, and those from the TOH to the MM, are slightly diachronous events. The lower part of the TOH of western sections is a time-equivalent of the uppermost Bellerophon Limestone in eastern sections, whereas its middle and upper part changes laterally into the Mazzin Member facies.

Acknowledgements

This project was financially supported by the Deutsche Akademie der Naturforscher Leopoldina (BMBF-LPD 9901/ 8-38). The sampling in Iran, carried out by the second author, was supported by the Deutsche Forschungsgemeinschaft and by the Geological Survey of Iran in Tehran and Täbris, particularly by B. Hamdi, H. Partoazar and B. Sedghi. The

analytical work of C. Spötl and technical assistance of M. Wimmer is appreciated. We thank H. Strauss and P. Wignall for review of the manuscript.

References

ASSERETO, R., BOSELLINI, A., FANTINI SESTINI, N. & SWEET, W.C. (1973): The Permian-Triassic boundary in the Southern Alps (Italy). - (In: LOGAN, A.S. & HILLS, A.B. (Eds.): The Permian and Triassic systems and their mutual boundary), Mem. Canad. Soc. Petroleum Geol., **2**: 176-199, Calgary.

BAUD, A., MAGARITZ, M. & HOLSER, W.T. (1989): Permian-Triassic of the Tethys: Carbon isotope studies. - Geol. Rundsch., **78**: 649-677, Stuttgart.

BERNER, R.A. (2002): Examination of hypotheses for the Permo-Triassic boundary extinction by carbon cycle modeling. - Proc. Natl. Acad. Sci. USA, **99**: 4172-4177, Washington.

BOWRING, S.A., ERWIN, D.H., JIN, Y.G., MARTIN, M.W., DAVIDEK, K. & WANG, W. (1998): U/Pb zircon geochronology and tempo of the end-Permian mass extinction. - Science, **280**: 1039-1045, Washington.

BRANDNER, R. (1988): The Permian-Triassic boundary in the Dolomites (Southern Alps, Italy), San Antonio section. - In: IGCP-Project 199: „Rare events in geology". Ber. Geol. Bundesanstalt, **15**: 49-56, Wien.

BROGLIO LORIGA, C., NERI, C., PASINI, M. & POSENATO, R. (1986): The upper Bellerophon Fm. and the P/T boundary, northern slope of the Sass de Putia Mt. - (In: Italian IGCP 203 Group (Eds.): Field Conference on Permian and Permian-Triassic boundary in the south-Alpine segment of the western Tethys (July 4 - 12, 1986), Field Guide-Book, 1st Edition) 82-88, (Società Geologica Italiana) Brescia.

BURKE, W.H., DENISON, R.E., HETHERINGTON, E.A., KOEPNICK, R.B., NELSON, H.F. & OTTO, J.B. (1982): Variation of seawater $^{87}Sr/^{86}Sr$ throughout Phanerozoic time. - Geology **10**: 516-519, Boulder.

CHEN, J., CHU, X., SHAO, M. & ZHONG, H. (1991): Carbon isotope study of the Permian-Triassic boundary sequences in China. - Chem. Geol., **86**: 239-251, Amsterdam.

CLAYPOOL, G.E., HOLSER, W.T., KAPLAN, I.R., SAKAI, H. & ZAK, I. (1980): The age curves of sulfur and oxygen isotopes in marine sulfate and their mutual interpretation. - Chem. Geol., **28**: 199-260, Amsterdam.

DE WIT, M.J., GHOSH, J.G., DE VILLIERS, S., RAKOTOSOLOFO, N., ALEXANDER, J., TRIPATHI, A. & LOOY, C. (2002): Multiple Organic carbon isotope reversals across the Permian-Triassic boundary of terrestrial Gondwana Sequences: Clues to extinction patterns and delayed ecosystem recovery. - J. Geol., **110**: 227-240, Chicago.

DETRE, C.H., BRAUN, T. & DON, G. (2002): New P/T interstellar sphaerule occurrences in the Bükk mts. (NE Hungary). - (In: ÈADA, M., HOUZAR, S., HRAZDÍL, V. & SKÁLA, R. (Eds.): IX. International Conference on moldavites, tektite and impact processes) Field trip guidebook and abstracts, **50**: Frantiskovy Lázne.

DOLENEC, T., LOJEN, S. & RAMOVŠ, A. (2001): The Permian-Triassic boundary in Western Slovenia (Idrijca Valley section): Magnetostratigraphy, stable isotopes, and elemental variations. - Chem. Geol., **175**: 175-190, Amsterdam.

ERWIN, D.H. (1993): The Permo-Triassic extinction. - Nature, **367**: 231-236, London.

ERWIN, D.H., BOWRING, S.A. & JIN, Y. (2002): End-Permian mass extinctions: A review. - (In: KOEBERL, C. & MACLEOD, K.G. (Eds.): Catastrophic events and mass extinctions: Impacts and beyond.) - Geol. Soc. Am. Spec. Pap., **356**: 363-383, Boulder.

FARABEGOLI, E. & PERRI, M.C. (1998): Stop 4.3 – Permian/Triassic boundary and Early Triassic of the Bulla section (Southern Alps, Italy): Lithostratigraphy, facies and conodont biostrati-graphy. - Giorn. Geol. Ser. 3ª (spec. issue, ECOS VII Southern Alps Fieldtrip Guidebook), **60**: 292-311, Bologna.

HANSEN, H.J., LOJEN, S., TOFT, P., TONG, J., MICHAELSEN, P. & SARKAR, A. (2000): Magnetic susceptibility and organic carbon isotopes of sediments across some marine and terrestrial Permo-Triassic boundaries. (In: YIN, H., DICKINS, J.M., SHI, G. & TONG, J. (Eds.): Permian-Triassic evolution of Tethys and western Circum-Pacific) Developments in Palaeontology and Stratigraphy, **18**: 271-289, Amsterdam.

HEYDARI, E, WADE, W.J. & HASSANZADEH, J. (2001): Diagenetic origin of carbon and oxygen isotope compositions of Permian-Triassic boundary strata. - Sed. Geol., **143**: 191-197, Amsterdam.

HOLSER, W.T. (1997): Geochemical events documented in inorganic carbon isotopes. - Palaeogeogr. Palaeoclimatol. Palaeoecol., **132**: 173-182, Amsterdam.

HOLSER, W.T. & KAPLAN, I.R. (1966): Isotope geochemistry of sedimentary sulfates. - Chem. Geol., **1**: 93-135, Amsterdam.

HOLSER, W.T. & MAGARITZ, M. (1987): Events near the Permian-Triassic boundary. - Mod. Geol., **11**: 155-180, Newark.

HOLSER, W.T. & MAGARITZ, M. (1992): Cretaceous / Tertiary and Permian / Triassic boundary events compared. - Geochim. Cosmochim. Acta, **56**: 3297-3309, New York.

HOLSER, W.T., SCHÖNLAUB, H.-P., ATTREP, M., BOECKELMANN, K., KLEIN, P., MAGARITZ, M., ORTH, C.J., FENNINGER, A., JENNY, C., KRALIK, M., MAURITSCH, H., PAK, E., SCHRAMM, J.-M., STATTEGGER, K. & SCHMÖLLER, R. (1989): A unique geochemical record at the Permian/Triassic boundary. - Nature, **337**: 39-44, London.

HUCKRIEDE, R. (1958): Die Conodonten der mediterranen Trias und ihr stratigraphischer Wert. - Paläont. Z., **32(3/4)**: 141-175, Berlin-Stuttgart.

JIN, Y.G., WANG, Y., WANG, W., SHANG, Q.H., CAO, C.Q. & ERWIN, D.H. (2000): Pattern of marine mass extinction near the Permian-Triassic boundary in South China. - Science, **289**: 432-436, Washington.

KOEPNICK, R.B., DENISON, R.E., BURKE, W.H., HETHERINGTON, E.A. & DAHL, D.A. (1990): Construction of the Triassic and Jurassic portion of the Phanerozoic curve of seawater $^{87}Sr/^{86}Sr$. - Chem. Geol., **80**: 327-349, Amsterdam.

KNOLL, A.H., BAMBACH, R.K., CANFIELD, D.E., & GROTZINGER, J.P. (1996): Comparative Earth history and late Permian mass extinction. - Science, **273**:452-457, Washington.

KORTE, C., KOZUR, H.W., BRUCKSCHEN, P. & VEIZER, J. (2003): Strontium isotope evolution of Late Permian and Triassic seawater. - Geochim. Cosmochim. Acta, **67**: 47-62, New York.

KORTE, C., KOZUR, H.W., JOACHIMSKI, M.M., STRAUSS, H., VEIZER, J. & SCHWARK, L. (2004a): Carbon, sulfur, oxygen and strontium isotope records, organic geochemistry and biostratigraphy across the Permian/Triassic boundary in Abadeh, Iran. - Int. J. Earth Sci. **93**: 565-581, Berlin-Heidelberg.

KORTE, C., KOZUR, H.W. & MOHTAT-AGHAI P. (2004b): Dzhulfian to lowermost Triassic $\delta^{13}C$ record at the Permian/Triassic boundary section at Shahreza, Central Iran. - Hallesches Jahrb. Geowiss. B, Beiheft **18**: 73-78, Halle (Saale).

KORTE, C., KOZUR, H.W. & PARTOAZAR, H. (2004c): Negative carbon isotope excursion at the Permian/Triassic boundary section at Zal, NW-Iran. - Hallesches Jahrb. Geowiss. B, Beiheft **18**: 69-71, Halle (Saale).

KOZUR, H. (1988): The Permian of Hungary. - Z. geol. Wiss., **16**(11/12): 1107-1115, Berlin.

KOZUR, H.W. (1991): Permian deep-water ostracods from Sicily (Italy). Part 2: Biofacial evaluation and remarks to the Silurian to Triassic palaeopsychrospheric ostracods. - Geol. Paläont. Mitt. Innsbruck, Sonderbd., **3**: 25-38, Innsbruck.

KOZUR, H.W. (1994): The correlation of the Zechstein with the marine standard. - Jb. Geol. B.-A., **137**: 85-103, Wien.

KOZUR, H.W. (1985): Neue Ostracoden-Arten aus dem oberen Mittelkarbon (höheres Moskovian), Mittel- und Oberperm des Bükk-Gebirges (N-Ungarn). - Geol. Paläont. Mitt. Innsbruck, Sonderband, **2(1)**: 1-145, Innsbruck.

KOZUR, H.W. (1998a): Some aspects of the Permian-Triassic boundary (PTB) and of the possible causes for the biotic crisis around this boundary. - Palaeogeogr. Palaeoclimatol. Palaeoecol. **143**: 227-272, Amsterdam.

KOZUR, H.W. (1998b): Problems for evaluation of the scenario of the Permian-Triassic boundary biotic crisis and of its causes. - Geol. Croat., **51/2**: 135-162, Zagreb.

KOZUR, H.W. (2004): Pelagic uppermost Permian and the Permian-Triassic boundary conodonts of Iran. Part I: Taxonomy. - Hallesches Jahrb. Geowiss. B, Beiheft **18**: 39-68, Halle (Saale).

KOZUR, H.W. (in press): Pelagic uppermost Permian and the Permian-Triassic boundary conodonts of Iran. Part II: Investigated sections and evaluation of the conodont faunas. - Hallesches Jahrb. Geowiss. B., Halle (Saale).

KOZUR, H.W., LEVEN, E.J., LOZOVSKIJ V.R. & PJATAKOVA M.V. (1978): Rasclenenie po konodontam pogranicnych sloev permi i triasa Zakavkazja. - Bjul. MOIP, otd. geol., **1978(5)**: 15-24, Moskau.

KOZUR, H.W. & MOCK, R. (1977): Conodonts and Holothurian sclerites from the Upper Permian and Triassic of the Bükk Mountains (North Hungary). - Acta Min.-Petr., **23(1)**: 109-126, Szeged.

KOZUR, H.W., MOSTLER, H. & RAHIMI-YAZD, A. (1975): Beiträge zur Mikropaläontologie permotriadischer Schichtfolgen. Teil II: Neue Conodonten aus dem Oberperm und der basalen Trias von Nord- und Zentraliran. - Geol.-Paläont. Mitt. Innsbruck, **5(3)**: 1-23, Innsbruck.

KRULL, E.S., RETALLACK, G.J., CAMPBELL, H.J. & LYON, G.L. (2000): ä$^{13}C_{org}$ chemostratigraphy of the Permian-Triassic boundary in the Maitai Group, New Zealand: Evidence for high-latitudinal methane release. - New Zeal. J. Geol. Geophys., **43**: 21-32, Wellington.

KUMP, L.R. (2003): The geochemistry of mass extinction, pp. 351-367. - (In: MACKENZIE, F.T. (Ed.) Sediments, diagenesis, and sedimentary rocks Vol. 7). Treatise of Geochemistry (Eds.): HOLLAND H.D. & TUREKIAN K.K.). Elsevier-Pergamon, Amsterdam.

MAGARITZ, M. (1989): ^{13}C minima follow extinction events: A clue to faunal radiation. - Geology, **17**: 337-340, Boulder.

MAGARITZ, M., BÄR, R., BAUD, A. and HOLSER, W.T. (1988): The carbon-isotope shift at the Permian/Triassic boundary in the Southern Alps is gradual. - Nature, **331**: 337-339, London.

MARTIN, E.E. & MACDOUGALL, J.D. (1995): Sr and Nd isotopes at the Permian/Triassic boundary: A record of climate change. - Chem. Geol., **125**: 73-99, Amsterdam.

MORANTE, R. (1996): Permian and Early Triassic isotopic records of carbon and strontium in Australia and a scenario of events about the Permian–Triassic boundary. - Historical Biology **11**: 289-310, Chur-London.

MOSTLER, H. (1982): Bozener Quarzporphyr und Werfener Schichten. - (In: Exkursionsführer zur 4. Jahrestagung der Österreichischen Geologischen Gesellschaft, Seis am Schlern, Südtirol, 1982) 43-79, Innsbruck.

MUSASHI, M., ISOZAKI, Y., KOIKE, T. & KREULEN, R. (2001): Stable carbon isotope signature in mid-Panthalassa shallow-water carbonates across the Permo–Triassic boundary: Evidence for ^{13}C-depleted superocean. - Earth Planet. Sci. Lett. **191**: 9-20, Amsterdam.

NERI, C. (1999): The P/T boundary in the Tesero section, western Dolomites (Trento), 3.2. Lithology and sedimentology. - (In: Stratigraphy and facies of the Permian deposits between Eastern Lombardy and the western Dolomites. Field Trip Guidebook of the Continental Permian International Congress, 15-25 September 1999, Brescia, Italy) 90-97, (Pavia University), Pavia.

NERI, C. & POSENATO, R. (1985): Litostratigrafia e macrofaune della Formazione a Bellerophon di Sass da Putia (Bolzano). - (In: COCOZZA, T. & RICCI, C.A. (Eds.): Evoluzione Stratigrafica, Tettonica, Metamorfismo e Magmatismo del Paleozoico italiano) 54-56, Ferrara.

NEWTON, R.J., PEVITT, E.L., WIGNALL, P.B. & BOTTRELL, S.H. (2004): Large shifts in the isotopic composition of seawater sulphate across the Permo–Triassic boundary in northern Italy. - Earth Planet. Sci. Lett. **218**: 331-345, Amsterdam.

NICORA, A. & PERRI, M. C. (1999): The P/T boundary in the Tesero section, western Dolomites (Trento), 3.3 Bio- and chronostratigraphy. - (In: Stratigraphy and facies of the Permian deposits between Eastern Lombardy and the western Dolomites. Field Trip Guidebook of the Continental Permian International Congress, 15-25 September 1999, Brescia, Italy) 97-100, (Pavia University), Pavia.

NOÉ, S.U. (1987): Facies and Paleogeography of the marine Upper Permian and of the Permian-Triassic boundary in the Southern Alps (Bellerophon Formation, Tesero Horizon). - Facies, **16**: 89-142, Erlangen.

OBERHÄNSLI, H., HSÜ, K.J., PIASECKI, S. & WEISSERT, H. (1989): Permian-Triassic carbon-isotope anomaly in Greenland and in the Southern Alps. - Historical Biology, **2**: 37-49, Chur-London.

PERRI M.C. (1991): Conodont biostratigraphy of the Werfen Formation (Lower Triassic), Southern Alps, Italy. - Boll. Soc. Paleont. It., **30**: 23-46, Modena.

RAUP, D.M. (1991): A kill curve for Phanerozoic marine species. - Paleobiology, **17**: 37-48, Lawrence.

RENNE, P.R., ZICHAO, Z., RICHARDS, M.A., BLACK, M.T. & BASU, A.R. (1995): Synchrony and causal relations between Permian-Triassic boundary crises and Siberian flood volcanism. - Science, **269**: 1413-1416, Washington.

SCHINDEWOLF, O.H. (1953): Über die Faunenwende vom Paläozoikum zum Mesozoikum. - Z. Dt. Geol. Ges. **105**: 153-182, Hannover.

SCHOLGER, R., MAURITSCH, H.J. & BRANDNER, R. (2000): Permian-Triassic boundary magnetostratigraphy from the Southern Alps (Italy). - Earth Planet. Sci. Lett., **176**: 495-508, Amsterdam.

SEPKOSKI, J.J. (1989): Periodicity in extinction and the problem of catastrophism in the history of life. - J. Geol. Soc. London, **146**: 7–19, London.

SPÖTL, C. & VENNEMANN, T.W. (2003): Continuous-flow isotope ratio mass spectrometric analysis of carbonate minerals. - Rapid Commun. Mass Spectrom. **17**: 1004-1006.

STAESCHE, U. (1964): Conodonten aus dem Skyth von Südtirol. - N. Jb. Geol. Paläont., **119(3)**: 247-306, Stuttgart.

STAMPFLI G.M. & BOREL G.D. (2002): A plate tectonic model for the Paleozoic and Mesozoic constrained by dynamic plate boundaries and restored synthetic oceanic isochrons. - Earth Planet. Sci. Lett. **196**, 17-33, Amsterdam.

STEPANOV, D.L., GOLSHANI, F. & STÖCKLIN, J. (1969): Upper Permian and Permian-Triassic boundary in North Iran. - Geol. Surv. Iran, Report, **12**: 1-72, Teheran.

SWEET, W.C. & MEI, S. (1999a): The Permian Lopingian and basal Triassic sequences in northwest Iran. - Permophiles, **33**: 14-20, Calgary.

SWEET, W.C. & MEI, S. (1999b): Conodont succession of Permian Lopingian and basal Triassic in northwest Iran. - (In: YIN, H. & TONG, J. (Eds.): Proceedings on the International Conference on Pangea and the Paleozoic-Meoszoic transition) 43-47, (China University of Geosciences Press), Wuhan.

TEICHERT, C., KUMMEL, B. & SWEET, W.C. (1973): Permian-Triassic strata, Kuh-E-Ali Bashi, northwestern Iran. - Bulletin of the Museum of Comparative Zoology, **145(8)**: 359-472, Cambridge, Mass.

VEIZER, J. & COMPSTON, W. (1974): $^{87}Sr/^{86}Sr$ composition of seawater during the Phanerozoic. - Geochim. Cosmochim. Acta, **38**: 1461-1484, New York.

VEIZER, J., ALA, D., AZMY, K., BRUCKSCHEN, P., BUHL, D., BRUHN, F., CARDEN, G.A.F., DIENER, A., EBNETH, S., GODDÉRIS, Y., JASPER, T., KORTE, C., PAWELLEK, F., PODLAHA, O.G. & STRAUSS, H. (1999): $^{87}Sr/^{86}Sr$, $\delta^{13}C$ and $\delta^{18}O$ evolution of Phanerozoic seawater. - Chem. Geol., **161**: 59-88, Amsterdam.

VISSCHER, H., BRINKHUIS, H., DILCHER, D.L., ELSIK, W.C., ESHET, Y., LOOY, C.V., RAMPINO, M.R., TRAVERSE, A. (1996): The terminal Paleozoic fungal event: Evidence of terrestrial ecosystem desta-

bilization and collapse. - Proc. Natl. Acad. Sci. USA, **93**: 2155-2158, Washington.

WANG, K., GELDSETZER, H.H.J. & KROUSE, H.R. (1994): Permian-Triassic extinction: Organic $\delta^{13}C$ evidence from British Columbia, Canada. - Geology, **22**: 580-584, Boulder.

WIGNALL, P.B., & HALLAM, A. (1992): Anoxia as a cause of the Permian/Triassic mass extinction: Facies evidence from northern Italy and the western United States. - Palaeogeogr. Palaeoclimatol. Palaeoecol., **93**: 21-46, Amsterdam.

WIGNALL, P.B., MORANTE, R. & NEWTON, R. (1998): The Permo-Triassic transition in Spitsbergen: $\delta^{13}C_{org}$ chemostratigraphy, Fe and S geochemistry, facies, fauna and trace fossils. - Geol. Mag., **135**: 47-62, Cambridge.

XU, D. & YAN, Z. (1993): Carbon isotope and iridium event markers near the Permian/Triassic boundary in the Meishan section, Zhejiang province, China. - Palaeogeogr. Palaeoclimatol. Palaeoecol., **104**: 171-176, Amsterdam.

YIN, H. & ZHANG. K. (1996): Eventostratigraphy of the Permian-Triassic boundary at Meishan section, South China. - (In: YIN, H. (Ed.): The Palaeozoic-Mesozoic boundary. Candidates of global stratotype section and point of the Permian-Triassic boundary), 84-96 (China University of Geosciences Press), Wuhan.